

SCIENTIFIC REPORTS



OPEN

Dose-dependent effects of chronic alcohol drinking on peripheral immune responses

Suhas Sureshchandra¹, Anthony Raus¹, Allen Jankeel¹, Brian Jin Kee Ligh², Nicole A. R. Walter³, Natali Newman³, Kathleen A. Grant³ & Ilhem Messaoudi^{1,3}

It is well established that chronic heavy alcohol drinking (CHD) results in significant organ damage, increased susceptibility to infections, and poor outcomes following injury. In contrast, chronic moderate drinking (CMD) has been associated with improved cardiovascular health and immunity. These differential outcomes have been linked to alterations in both innate and adaptive branches of the immune system; however, the mechanisms remain poorly understood. To address this question, we determined the impact of chronic drinking on the transcriptional and functional responses of peripheral blood mononuclear cells (PBMC) collected from male rhesus macaques classified as CMD or CHD after 12 months of voluntary ethanol self-administration. Our analysis suggests that chronic alcohol drinking, regardless of dose alters resting transcriptomes of PBMC, with the largest impact seen in innate immune cells. These transcriptional changes are partially explained by alterations in microRNA profiles. Additionally, chronic alcohol drinking is associated with a dose dependent heightened inflammatory profiled at resting and following LPS stimulation. Moreover, we observed a dose-dependent shift in the kinetics of transcriptional responses to LPS. These findings may explain the dichotomy in clinical and immunological outcomes observed with moderate versus heavy alcohol drinking.

Observational studies in humans have reported strong associations between chronic heavy drinking (CHD) and significant organ damage as indicated by increased incidence of acute respiratory stress syndrome (ARDS)¹, alcoholic liver disease (ALD)², certain cancers^{3–5}, cardiovascular diseases^{6,7}, and sepsis⁸. Moreover, CHD results in increased susceptibility to pneumonia^{9,10}, tuberculosis^{11–13}, and faster progression of hepatitis C virus (HCV)¹⁴ and HIV infections¹⁵. Furthermore, individuals who engage in CHD exhibit higher rates of postoperative complications¹⁶, slower recovery from infection and trauma¹⁶, poor vaccine responses¹⁷, and wound healing¹⁸. In contrast, chronic moderate drinking (CMD) has been associated with decreased cardiovascular disease, improved insulin sensitivity, and decreased incidence of the common cold in humans^{19–21}.

These studies suggest that chronic moderate and heavy drinking exert opposing effects on the human immune system; however, the mechanisms by which chronic drinking modulates immunity remain poorly understood. The earliest studies on CHD suggested that long-term drinking (several years to decades) is associated with reduction in T-cell numbers²², loss of naïve T-cells^{22,23}, increased CD8+ T-cell activation and proliferation²⁴, and increased serum immunoglobulin levels²⁵. CHD also results in higher levels of circulating pro-inflammatory mediators TNF α , IL-1 β , and IL-6²⁶. Interpretation of these clinical studies are however confounded by age, erratic drinking patterns, sex, smoking status, use of recreational or illicit drugs, and nutritional deficiencies.

More recent *in vitro* studies where peripheral blood mononuclear cells (PBMC) isolated from healthy humans (not meeting the criteria of CHD) or monocytic cell lines were cultured with ethanol suggest that short (hours) and long-term (days) exposure have opposing effects on inflammatory responses of innate immune cells²⁷. Specifically, while short-term exposure increased production of regulatory cytokines (e.g. IL-10) and decreased production of pro-inflammatory factors (TNF α and IL-6)^{28–30}, long-term exposure heightened TNF α secretion following stimulation with toll-like receptor (TLR) 4 and 8 ligands^{29,31,32}. However, these *in vitro* studies do not take into account the effects of ethanol's metabolites and the pleiotropic impact of ethanol consumption on other immune cells, which can be modeled only using *in vivo* exposure.

¹Department of Molecular Biology and Biochemistry, University of California-Irvine, Irvine, CA, 92697, USA.

²Department of Biomedical Engineering, University of California-Irvine, 92697, Irvine, CA, USA. ³Oregon National Primate Research Center, Oregon Health & Science University, 97006, Beaverton, OR, USA. Correspondence and requests for materials should be addressed to I.M. (email: imessaou@uci.edu)

The inhibitory effect of acute ethanol on production of pro-inflammatory cytokines in response to a variety of microbial compounds has been recapitulated using mouse models of acute ethanol exposure (reviewed in^{27,33}). A handful of studies based in rodent models of chronic ethanol consumption have reported increased pathogen burden and impaired ability to clear *Listeria monocytogenes*³⁴, *Mycobacterium tuberculosis*³⁵, and influenza virus³⁶. On the other hand, moderate alcohol exposure can improve microbial clearance and delay cutaneous hypersensitivity responses in rodents³⁷. However, rodent studies employ gavage feeding, liquid diets, or intraperitoneal injections introducing other confounders such as nutritional status and nonvolitional stress for the animals. Finally, rodent models fail to recapitulate human patterns of light to moderate drinking.

To overcome these limitations, we used a rhesus macaque model of voluntary ethanol consumption established with a schedule-induced polydipsia procedure^{38–40}. In this model, rhesus macaques are first induced to self-administer increasing daily doses of ethanol (0.5 g/kg/day to 1.5 g/kg/day over a 90-day period), then allowed “open access” to both water and 4% w/v ethanol for 22 h/day. During the open access phase to the protocol, the monkeys self-select their drinking status (CHD or CMD). This model presents a unique opportunity to study the impact of chronic voluntary moderate/heavy drinking on immunity in a highly translational outbred animal model without any overt tissue damage. We have leveraged this model to define the impact of chronic drinking on circulating and tissue resident immune cells^{41–46}. Specifically, using this model, we have shown that CMD enhances while CHD attenuates vaccine responses^{42,44,47}. More recently, we reported significant transcriptional changes in PBMC from female rhesus macaque following 12 months of CHD using RNA-Seq and concluded that the circulating innate immune cells bear the largest burden of chronic heavy drinking⁴⁶. Therefore, in this study, we investigated the impact of both CHD and CMD on PBMC transcriptional profile and immune mediator production at resting and after stimulation with lipopolysaccharide (LPS) using samples obtained from three cohorts of male rhesus macaques that followed a standard protocol of daily open-access to 4% ethanol in water solution for over 12 months.

As previously reported with CHD females, we observe increased expression of genes in pathways regulating coagulation and inflammation with CHD, but not in CMD. Additionally, we observed a hyper-inflammatory phenotype both at resting and following LPS stimulation that was dose-dependent. Three-way comparison on RNA levels 16 hours post stimulation suggests that while transcriptional profile of PBMC from controls is suggestive of a sustained strong pro-inflammatory response, the transcriptional profile of PBMC from moderates indicates a return to baseline. PBMC from CHD animals, on the other hand, exhibited a transcriptional profile consistent with a regulatory phase of LPS response. These data strongly suggest a shift in inflammatory trajectory/timeline with chronic alcohol drinking.

Results

Chronic drinking alters transcriptional profiles of resting PBMC independent of ethanol dose. To assess the overall impact of chronic drinking on peripheral immune cells, we performed RNA-Seq on PBMC isolated from three control animals and eight animals categorized as “chronic moderate drinkers” (CMD) (n = 4) or “chronic heavy drinkers” (CHD) (n = 4) at the end of 12 months of ethanol self-administration (Supplementary Fig. 1a–c). Principal Component Analysis (PCA) of PBMC transcriptomes demonstrate a substantial effect of chronic drinking, where transcriptional profiles of samples obtained from CMD and CHD animals segregate away from those of control animals (Fig. 1a). Furthermore, alcohol is a strong determinant of resting PBMC transcriptome, demonstrated by reduced within group variability in gene expression profiles (Supplementary Fig. 2a). Differential gene expression analysis using edgeR (Supplementary Table 1) identified 452 and 338 differentially expressed genes (DEG; FDR ≤ 0.05) that were mostly upregulated with ethanol consumption in both CHD (410 of 452) and CMD (302 of 338) groups respectively relative to the control group (Fig. 1b) with a significant overlap between these two DEG subsets (p < 0.0001, hypergeometric test) (Fig. 1c). Limited gene expression changes were detected between the CMD and CHD groups, indicating that ethanol consumption is the major driver of these transcriptional changes (Fig. 1b). These differences were observed in the absence of any differences in immune cell frequencies among the three groups⁴³.

DEG (annotated protein coding and microRNA genes) detected only in CHD group enriched to gene ontology (GO) terms associated with inflammation (e.g., *CRP*, *ALOX5*, *TF*, *C1S*, and *C9*), signaling, and blood homeostasis (e.g. fibrinogen genes *FBA*, *FGB*, and *FGG* as well as wound healing factors *TBXA2R*, *SERPING1*, and *SERPINB2*) (Supplementary Fig. 2b). Additional analyses of protein-protein interactions indicate that DEG detected only in CHD group play a role in membrane trafficking, mitochondrial protein synthesis, as well as GPCR and TLR signaling pathways (Supplementary Fig. 2c). The DEG detected only in the CMD group were primarily involved in cellular chemical homeostasis (*SNCA*, *SLC4A1*, *SLC4A10*, *SLC35G1*), chemotaxis (*FPR3*, *C5AR2*, *GPR18*), and cytokine signaling (*CD200R1*, *NR1H3*, *ECM1*) (Supplementary Fig. 2d). The 193 DEG detected in both CMD and CHD groups relative to controls (Fig. 1c) enriched to GO terms associated primarily with metabolic pathways (Supplementary Fig. 2e).

In order to explore dose-dependent changes in gene expression, we next combined DEG detected in CHD and CMD relative to controls and modeled expression profiles of these genes using Short Time-series Expression Miner (STEM)⁴⁸, replacing time with ethanol dose as the independent variable. This analysis identified four significant clusters (p < 0.05) (Fig. 1d and Supplementary Fig. 2f) with distinct patterns of dose dependence. For example, expression levels of genes in cluster I increased with chronic drinking but reached higher levels in the CMD group (Fig. 1d and Supplement Fig. 2f). These DEG play a role in anion transport and cellular signaling (Fig. 1e). Cluster II contained DEG the expression of which only increased with CMD (Fig. 1d and Supplement Fig. 2f). These DEG are important for cellular metabolism and ECM-receptor interaction (*IL1R*, *ITGA9*, *FGG*) (Fig. 1e). Finally, expression of DEG in cluster III increased with CMD and plateaued, while expression of DEG in cluster IV progressively

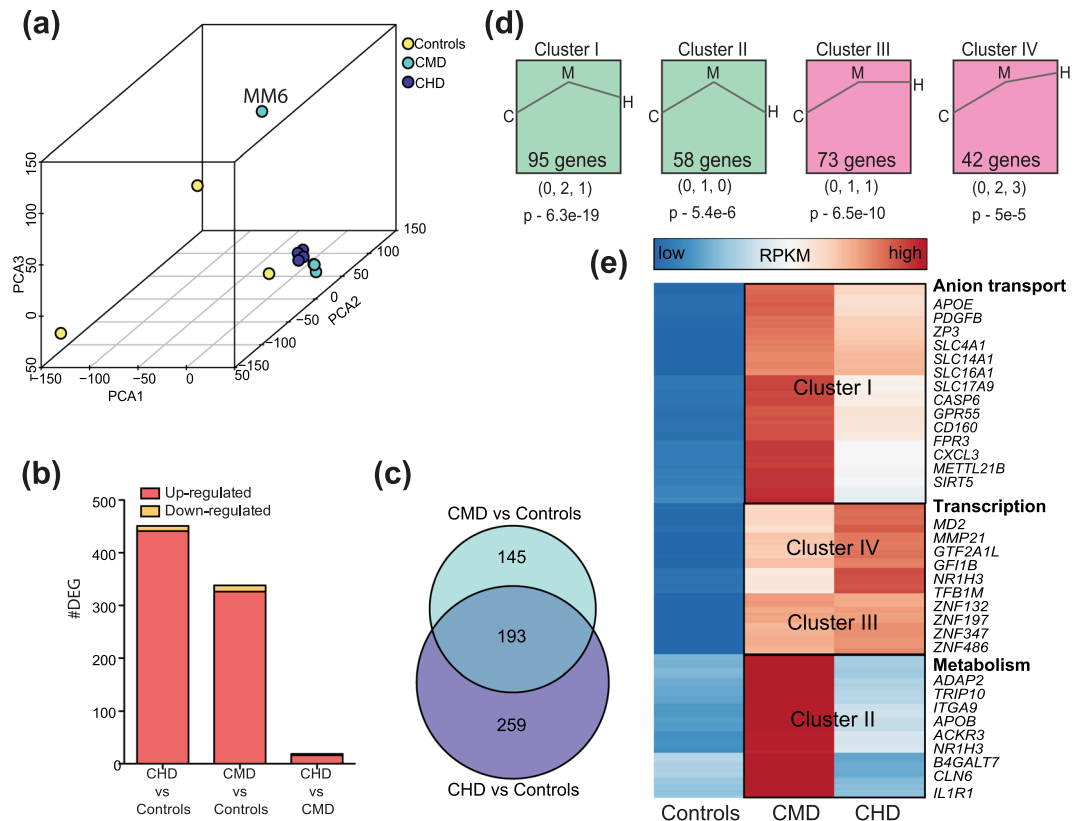


Figure 1. Chronic alcohol drinking alters PBMC gene expression independent of ethanol dose (a) 3D PCA of resting gene expression profiles of PBMC isolated from controls (n = 3), CMD (n = 4), and CHD (n = 4) animals. A potential outlier from CMD is highlighted but was retained in subsequent downstream analyses due to minimal changes in DEG profiles following its removal. (b) Bar graphs denoting number of differentially expressed genes (DEG) (protein coding and miRNA precursor) in CMD and CHD PBMC relative to control PBMC and each other. (c) Venn diagram describing overlap of DEG detected in CHD and CMD animals relative to controls. (d) Clusters of dose-dependent gene expression changes within the 597 genes dysregulated with chronic drinking (CMD and CHD combined) identified using STEM. Only statistically significant clusters ($p < 0.05$) are shown. Magnitudes of changes in controls (C), CMD (M), and CHD (H) are represented numerically below each representative cluster, with its statistical significance reported by STEM. (e) Heatmap of 268 ethanol sensitive DEG that demonstrated dose-dependent changes in expression (clusters I, II, III, and IV combined). Each row represents a gene with median expression level (RPKM) scaling from low (blue) to high (red). A subset of DEG within each cluster is highlighted.

increased with ethanol consumption. DEG in both of these clusters were involved in transcriptional regulation (several zinc finger proteins) and myeloid cell activation (*MD2*, *NR1H3*, and *MMP21*) (Fig. 1e).

To get a better understanding of the cellular sources of the DEG detected, we next used the ImmGen database⁴⁹, which visualizes the distribution of genes across immune cell populations to infer the source of the gene expression changes detected. In agreement with our previous study in CHD females⁴⁶, the majority of the DEG detected with both CMD and CHD are highly expressed by monocytes and dendritic cells (DCs) (Supplementary Fig. 3a,b).

CMD and CHD alter microRNA (miRNA) profiles of PBMC. Analysis of RNA-Seq data indicated changes in some microRNA (miRNA) precursors with both CHD and CMD. To gain a deeper understanding of the impact of drinking on miRNA expression patterns, we next profiled all cellular mature miRNA using an additional sequencing experiment (Supplementary Fig. 1c, Supplementary Table 2) (n = 4/group). We identified 534 macaque miRNAs with a median expression level (RPKM) > 1. To assess the role of miRNA in PBMC from rhesus macaques, we identified 8,856 validated gene targets for the 100 most highly expressed miRNAs from control animals using miRNet. Functional enrichment of these genes indicates that they play a role in pathogen sensing, response to infections, and adaptive immune signaling (Supplementary Fig. 4a).

Surprisingly, only 11 differentially expressed miRNA genes, which were mostly downregulated with drinking (9 of 11), were detected with CHD (Fig. 2a). Of the 452 mRNA DEG detected with CHD, 46 are validated targets of these differentially expressed mature and precursor miRNAs (Fig. 2b). Moreover, these 46 DEG play roles in regulation of body fluids, coagulation, and wound healing (Fig. 2c). On the other hand, CMD was associated with 24 differentially expressed miRNA, which were also mostly downregulated with drinking (19 of 24). These miRNA

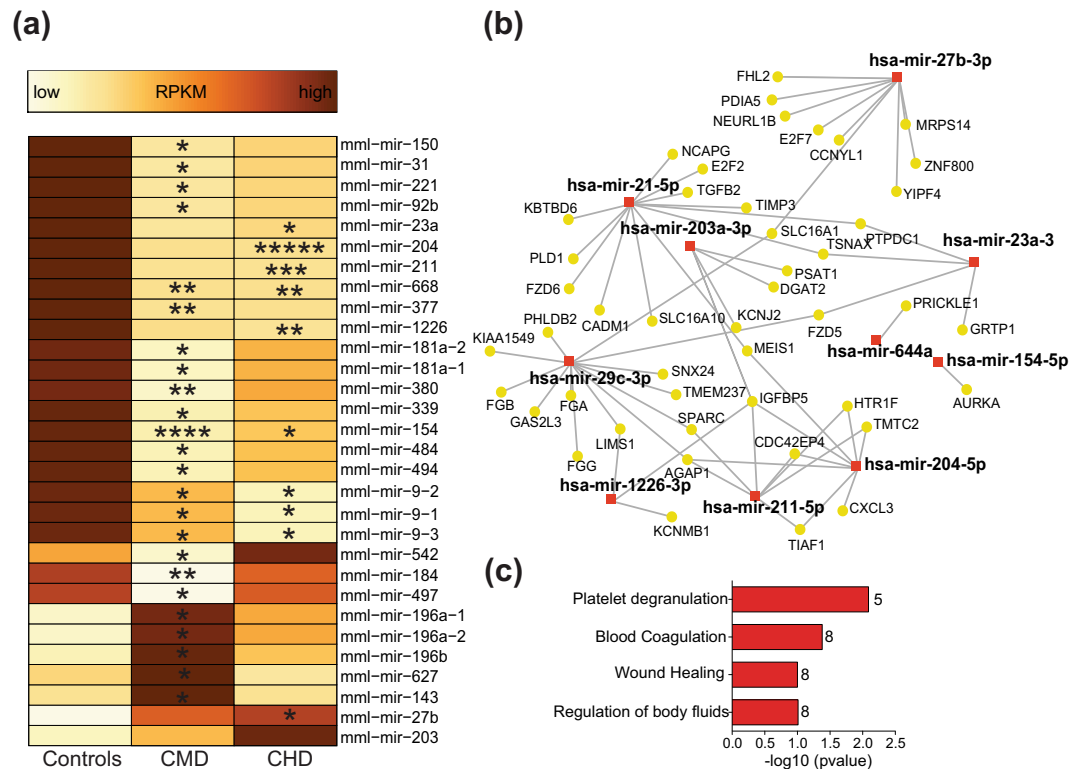


Figure 2. Chronic alcohol drinking alters microRNA profile of PBMC. **(a)** Heatmap showing median RPKM of ethanol sensitive mature microRNAs from controls (n = 4), CMD (n = 4), and CHD (n = 4) animals detected using small RNA sequencing. Colors represent median transcript levels (RPKM) scaled from low (yellow) to high (brown). Asterisks indicate levels of statistical significance relative to controls: *p ≤ 0.05; **p ≤ 0.01; ***p ≤ 0.001; ****p ≤ 0.0001. **(b)** Network of miRNAs dysregulated with CHD (red squares) and their validated mRNA targets that are dysregulated with CHD (yellow circles) built using miRNet. **(c)** Functional enrichment of the targets highlighted in **(b)** predicted using Reactome and GO database in miRNet. (P-values were derived from hypergeometric tests). Numbers next to the bar denote genes mapping to each functional enrichment term.

(Fig. 2a) were associated with 60 validated gene targets within the 338 mRNA DEG with CMD (Supplementary Fig. 4b). Finally, different microRNA were upregulated with CMD (miR-196, miR-143, and miR-627) and CHD (miR-27b and miR-203).

Chronic drinking alters the immune response to LPS in a dose-dependent manner. Given that the majority of transcriptional changes are predicted to originate from monocytes and DCs (Supplementary Fig. 3a,b), we next determined if chronic drinking results in altered responses to TLR ligands. PBMC from control (n = 4), CMD (n = 4), and CHD (n = 4) animals were cultured for 16 hours in the presence or absence of TLR4 agonist LPS (Fig. 3a). We then measured differences in immune mediator production using a multiplex bead array and changes in gene expression using RNA-Seq (Fig. 3a). First, we assessed the impact of chronic drinking on spontaneous immune mediator production using principal component analyses (PCA), which revealed distinct resting cytokine profiles (Fig. 3b) (Supplementary Table 3). Additionally, we measured the relationship between secreted levels of analytes and ethanol dose using linear regression (Fig. 3c and Supplementary Fig. 5a). This analysis revealed a dose dependent increase in spontaneous production of inflammatory cytokines IFN γ (p = 3e-3), IL-15 (p = 2e-2), IL-2 (p = 5e-4), TNF α (p = 0.05), and IL-1 β (p = 0.05); growth factors HGF (p = 2e-3) and FGF-2 (p = 0.01); and chemokines IL-8 (p = 1e-4) (Fig. 3c and Supplementary Fig. 5a). Interestingly, we observed a dose-dependent reduction in spontaneously secreted levels of RANTES (p = 4e-3) (Fig. 3c and Supplementary Fig. 5c).

Following LPS stimulation, we observed a dose-dependent increase in IFN γ (p = 9e-3), IL-8 (p < 0.0001), and HGF (p = 0.03) secretion with chronic drinking (Fig. 3c and Supplementary Fig. 5b). Additionally, we observed a linear trend in post LPS IL-1 β induction with ethanol dose (p = 0.1) (Supplementary Fig. 5c). As described above for spontaneous production, we noted a dose-dependent reduction in post LPS induction of RANTES (p = 0.02) as well as MIP-1 β (p = 0.01) (Fig. 3c and Supplementary Fig. 5c).

Chronic drinking alters transcriptional responses to LPS in a dose-dependent manner. We next determined if alterations in the response to LPS with chronic drinking were recapitulated at the transcriptional level (Supplementary Table 4). In contrast to the control group where we observed a strong induction of a gene expression at 16 hours (362 DEG), we detected limited transcriptional changes in the CMD group (10 DEG), and down-regulation of 86 DEG in CHD (Fig. 4a), 44 of which were also detected in controls (Fig. 4b). DEG

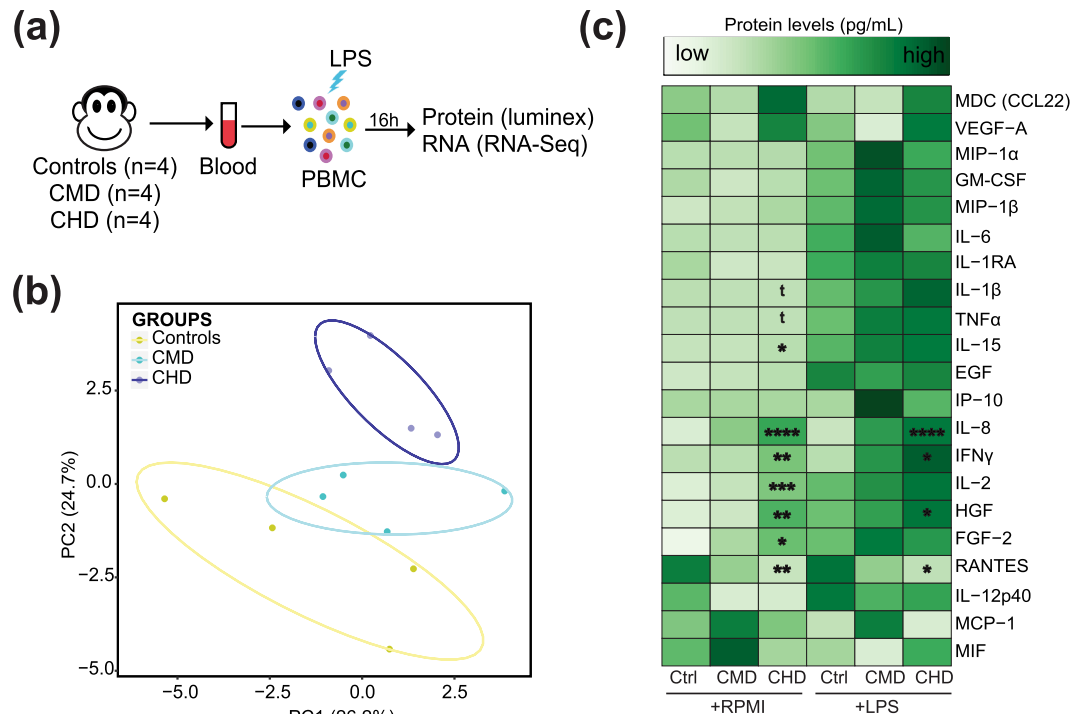


Figure 3. Chronic alcohol drinking alters immune responses to LPS. **(a)** Experimental design: PBMC from controls (n = 4), CMD (n = 4), and CHD (n = 4) animals were cultured in the presence or absence of LPS for 16 h. Supernatants were collected for immune mediator measurements using multiplex bead assay and the cell pellets were used for RNA extraction and RNA-Seq. **(b)** Principal Component Analysis (PCA) of overall immune mediator profiles (21 analytes detected above limits of detection) produced in the absence of LPS stimulation. Each circle represents a biological sample. **(c)** Heatmap of median secreted analyte concentrations (pg/mL) before and after LPS stimulation. Dose associated linear increases or decreases in secreted levels both before and after stimulation were independently tested using linear regression analysis. Analytes with statistically significant and trending linear association with ethanol consumption dose are marked (t - p = 0.05; *p ≤ 0.05; **p ≤ 0.01; ***p ≤ 0.001; ****p ≤ 0.001, F-tests). Protein concentrations are scaled from low (light green) to high (dark green).

detected in control group only (Fig. 4b) played a role in canonical inflammatory response to LPS as indicated by functional enrichment to GO terms “innate immune response” and “cytokine signaling” as well as regulatory modules “mRNA metabolic process” and “chromatin reorganization” (Fig. 4c). Next, we explored potential dose dependent changes in gene expression changes. STEM analysis of all the 390 LPS-responsive DEG (Fig. 4b) identified four distinct but significant clusters (p < 0.001) (Fig. 4d). DEG in clusters I, II, and III displayed ethanol dose-dependent changes (Fig. 4d and Supplement Fig. 6). DEG in these 3 clusters played a role in inflammation (CD83, CD163), signaling (JAK1, STK4, PIK3R1) and cell adhesion (TMEM2, PTPN1, KTN1, SLK) (Fig. 4e). DEG in cluster IV were down regulated with drinking regardless of dose and are involved in transcriptional regulation (Fig. 4d,e).

Of the 44 DEG detected in both controls and CHD (Fig. 4b), 43 showed opposite directional changes (upregulated in controls but downregulated in CHD), and no change in expression in CMD (Fig. 5a). These genes play roles in cytokine signaling, leukocyte differentiation, and wound healing (Fig. 5b). More importantly, this list includes genes involved in sustaining cytokine production (JAK1, DOCK11, and PIK3R1) and cell surface receptors involved in activation (CD83), adhesion (ITGB1 which encodes VCAM1), and chemoattraction (CXCR4) (Fig. 5c). The largely downregulated DEG exclusively detected with CHD (Fig. 4a) played a role in myeloid leukocyte activation and regulation of stress response (Fig. 5d).

Discussion

In this study, we used a macaque model of voluntary ethanol self-administration to investigate the impact of CMD and CHD on the PBMC transcriptional profile and its response to LPS. Specifically, PBMC isolated from male rhesus macaques that were classified as controls or categorized as CMD or CHD based on their patterns of ethanol self-administration over a 12-month period were subjected to RNA-Seq and Luminex analysis before and after LPS stimulation. While there is a significant overlap between gene expression changes induced by CMD and CHD, transcriptional changes exclusively detected with CHD enriched to blood coagulation, immune signaling and wound healing pathways. This observation is in line with the increased susceptibility to cardiovascular disease^{6,7} and impaired wound healing^{16,18,50} observed in subjects with alcohol use disorder. CMD on the other hand triggers activation of cellular metabolic pathways with dose-associated increases in expression of genes involved in transcriptional regulation and myeloid cell activation. To our knowledge, this is the first report of

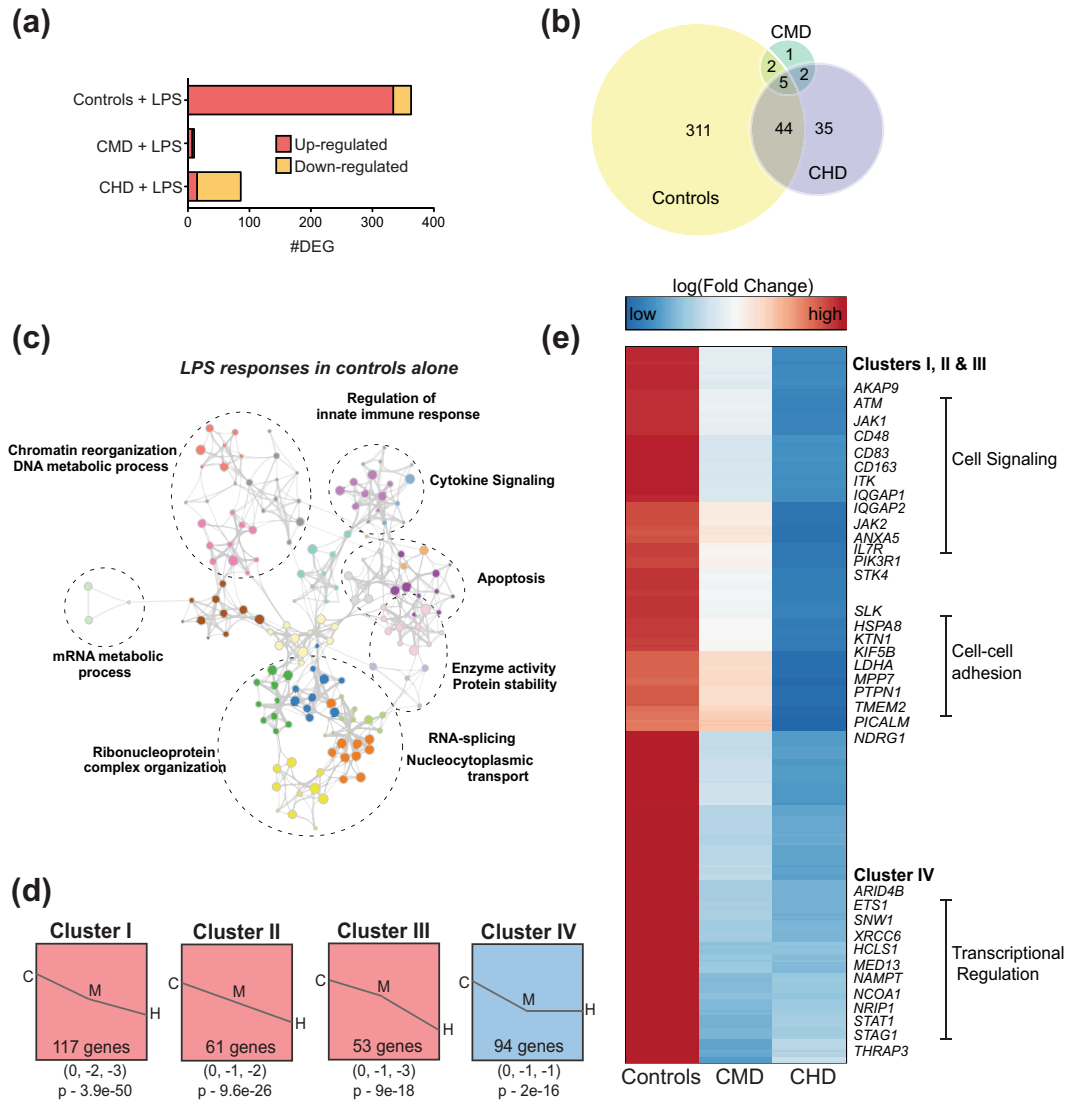


Figure 4. CMD and CHD exhibit distinct transcriptional responses to LPS in PBMC. **(a)** Bar graphs of protein coding DEG detected at 16 hours post LPS stimulation in PBMC from controls (n = 4), CMD (n = 4), and CHD (n = 4) animals. **(b)** 3-way Venn illustrating the overlap of DEG detected following LPS stimulation in controls, CMD and CHD. **(c)** Network of GO terms to which DEG detected in response to LPS in control group only (311 genes) generated using Metascape. Each bubble represents a GO term and clusters of similar GO terms are placed in bubbles delineated with dashed lines and labeled with the most statistically significant GO term. Size of the bubble represents number of genes mapping to the GO term and gray line indicate strength of association between different GO terms. **(d)** Modeling dose-dependent transcriptional responses to LPS using fold changes (log scale) of 400 genes identified in **(b)** using STEM. Only statistically significant clusters (p < 0.05) are shown. Magnitudes of fold changes in controls (C), CMD (M), and CHD (H) are represented numerically below each representative cluster, with its statistical significance reported by STEM. **(e)** Clustered heatmap of 325 genes that demonstrate dose dependent transcriptional responses to LPS (clusters I, II, III, and IV combined). Each row represents a gene with fold change (log scale) relative to unstimulated controls scaling from low (blue) to high (red). Subsets of genes within each cluster are highlighted.

transcriptional changes in resting immune cells with moderate drinking. Furthermore, profiling miRNA repertoire further indicates that the pro-inflammatory impact of drinking is significant only in CHD and not in CMD.

As we recently reported for gene expression changes of resting PBMC isolated from CHD female rhesus macaques⁴⁶, additional mining of data using online databases suggested that a majority of these transcriptional triggers in PBMC from both CMD and CHD originate from DCs and monocytes. Moreover, gene expression changes reported in this study of CHD males enrich to similar biological processes, notably immune signaling and coagulation pathways, as those reported for PBMC from CHD females⁴⁶. In both cases, these differences were observed in the absence of changes in frequencies of major circulating immune cells^{43,46} suggesting potential immune reprogramming with both CMD and CHD, most likely in innate immune cells. These observations are in line with previous reports of significant changes in innate immune branch within short period of

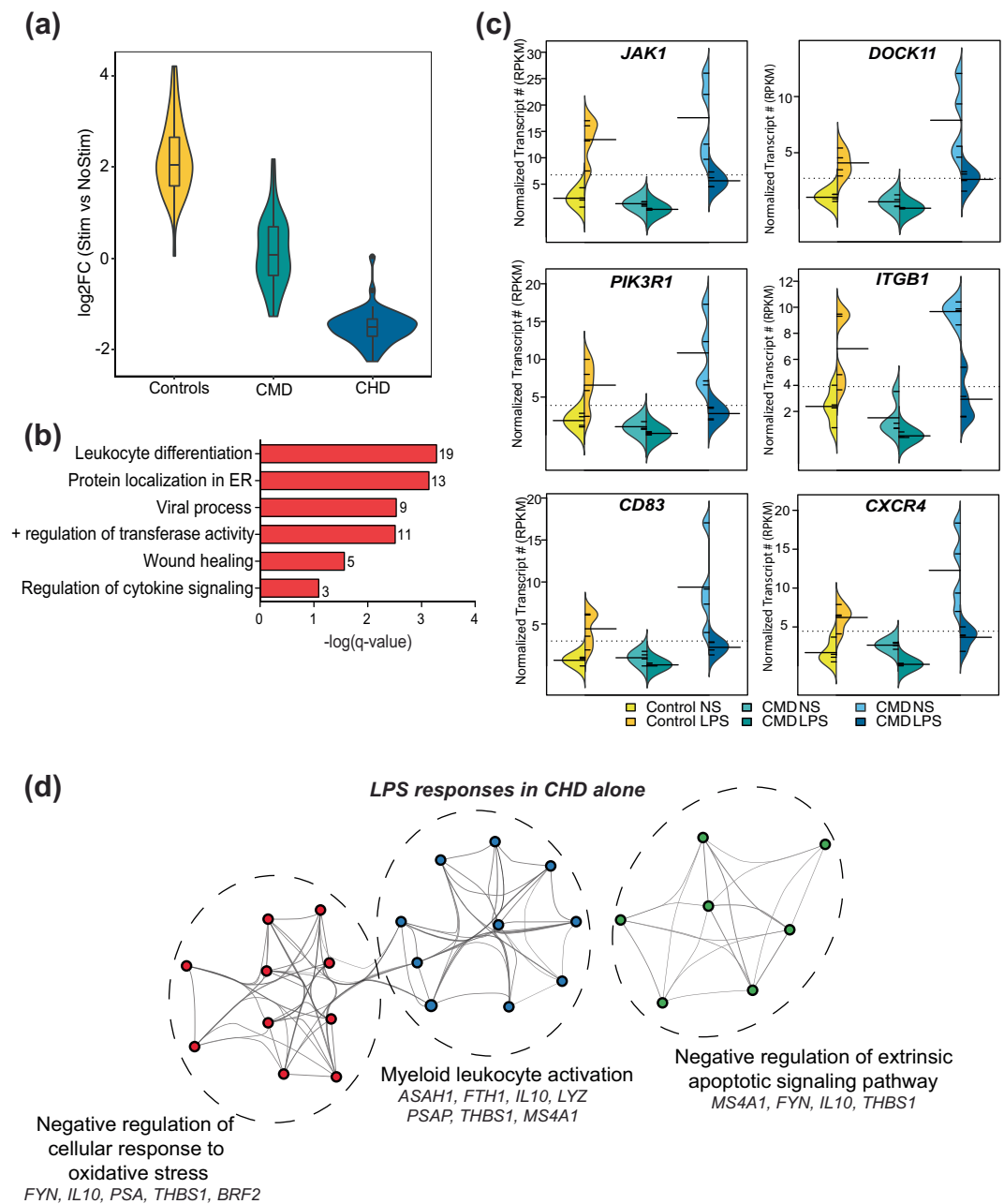


Figure 5. Dose-dependent transcriptional responses to LPS with chronic alcohol drinking. **(a)** Violin plot representing \log_2 Fold Change of the 44 DEGs detected in both CHD and control PBMC following LPS stimulation. **(b)** Functional enrichment of the 44 DEGs detected in both controls and CHD groups. Numbers next to the bar represent numbers of genes mapping to each term. **(c)** Bean plots of RPKM levels of select DEGs detected in both control and CHD animals. **(d)** Network depicting functional enrichment of the DEGs detected exclusively dysregulated in CHD following LPS stimulation identified using Metascape. Each colored bubble represents a GO term clustered within a dotted circle with annotations and genes mapping to the terms.

exposure to ethanol while changes in adaptive branch are often only detected after decades of alcohol dependence in humans or >6 months of chronic consumption of high concentration of ethanol solution in rodents (equivalent to 20 human years)⁴⁴.

The observation that ethanol sensitive gene expression changes enrich to pathways that regulate platelet degranulation and coagulation is consistent with the fact that alcohol use disorder interferes with several aspects of the blood clotting system, causing abnormally low platelet numbers in the blood, impaired platelet function, and diminished fibrinolysis⁵¹. Sex-specific differences in the impact of ethanol consumption on immune cells transcriptional profile may be attributed to differences in signaling by sex steroids. It is, however, important to note that some of the females from our previous study consumed higher average levels of ethanol over the 12 months of open access (range from 3.29–5.17 g/kg/day) than the CHD males in this study (range from

3.01–4.21 g/kg/day). Therefore, at this point we are unable to tease the impact of sex from those of ethanol dose on immunity.

Innate immune cells may be more sensitive to the impact of ethanol consumption due to their short half-life and rapid turnover production from the bone marrow. In contrast, lymphocytes are primarily produced during fetal development and are very long-lived. However, it is currently unclear whether this impact is mediated by ethanol metabolites acting on circulating myeloid cells or if ethanol reprograms the myeloid precursors in the bone marrow during their lineage development. The involvement of both mechanisms is highly likely since chronic binge drinking has been shown to impair activation of granulocyte precursor cells in response to bacteremia in mice⁵².

Given that both CMD and CHD exert a dramatic impact on myeloid cells, which play a critical role in wound healing and battling infections; we investigated changes in response to LPS as a model bacterial antigen. Previous *ex vivo* and *in vitro* studies have reported an exposure dependent change in the monocyte responses to LPS where acute exposure to ethanol is associated with dampened monocyte responses to LPS and prolonged exposure is associated with enhanced LPS response (reviewed in⁴⁴). However, these studies stimulated human PBMC or THP1/RAW cell lines with LPS for various durations in the presence of different amounts of ethanol and measured canonical LPS inducible cytokines as readouts. Furthermore, the impact of moderate and heavy drinking on LPS inducible transcriptional response was unknown.

At the protein level, linear regression analyses suggest strong dose dependence in the secretion of several pro-inflammatory factors and growth factors both under resting conditions (TNF α , IL-1 β , IFN γ , IL-2, FGF2, and HGF) and post LPS exposure (IL-8, RANTES, HGF, and IFN γ). These findings are in agreement with recent clinical studies that showed greater inflammatory mediator production by alveolar macrophages and PBMC obtained from human excessive/heavy alcohol consumers in response to LPS and lipoteichoic acid (LTA)⁵³. While post-LPS production of cytokines *ex vivo* is a measure of immunocompetence, spontaneous production of cytokines has been previously linked to a state of *in vivo* activation⁵⁴. Indeed, in line with this hypothesis, a recent report in humans suggested that the ethanol dose consumed positively correlated with serum markers of monocyte activation⁵⁵, providing a potential explanation for heightened pro-inflammatory responses to LPS in CHD. Interestingly, our analysis revealed dose-associated drop in spontaneously produced RANTES and post LPS induction of MIP-1 β . However, given that these *in vitro* experiments involved mixed populations of immune cells, it is hard to attribute this trend to reduced production or enhanced signaling of chemokine factors.

Several potential mechanisms could explain a state of heightened immune cell activation following chronic ethanol consumption. Alcohol has been shown to disrupt the gut intestinal epithelial barrier permeability^{56,57}, leaking microbial antigens and endotoxins into circulation in acute binge drinking models⁵⁸. In humans, long term drinking has been associated with higher serum endotoxin levels, which increase in a dose-dependent manner⁵⁵. Similarly, we have recently reported a dose-dependent increase in the levels of circulating IgM-bound endotoxin levels in the animals used in this study⁴⁵. It is, however, still unclear if ethanol-induced leakage of microbial antigens reprograms the bone marrow to influence hematopoiesis or acts on circulating immune cells. Aberrant activation of myeloid precursor cells would suggest that the effects of heavy drinking on the immune system are both long-term and irreversible.

A hyperactive resting state may interfere with the generation of appropriate responses to microbial antigens. To begin to address this question, we investigated the transcriptional response to LPS stimulation. RNA-Seq measurements in PBMC from control animals at 16 hours post stimulation indicate activation of canonical inflammatory pathways associated with an LPS response such as cytokine signaling and innate immune response; and regulatory mechanisms such as mRNA catabolism, translation, and apoptosis. In contrast, responses in CHD animals indicate down-regulation of several genes involved in leukocyte differentiation, wound healing, and cytokine signaling. These observations are suggestive of a resolution phase. This scenario is corroborated by up-regulation of *IL10*, essential for a strong anti-inflammatory response⁵⁹, in CHD animals only (Fig. 5d). It is possible that a heightened activation state of resting PBMC from CHD prevents them from further up-regulating expression of canonical pathways essential for the LPS response, suggestive of an immune tolerant phenotype.

Alterations in responses of PBMC from CHD to LPS can also be attributed to epigenetic changes. We have previously shown that ethanol sensitive miRNAs explain vaccine induced gene expression changes in PBMC⁴⁴. In this study, we report changes in expression of mature and precursor miRNA molecules, which have validated roles in LPS signaling (miR-21, miR-29, miR-211, and miR-204)^{60,61}. miR-204, for example, is a negative regulator of TLR4 signaling⁶² through its target *JAK2*. Decreased expression of miR-204 with CHD correlates with enhanced pro-inflammatory phenotype observed with CHD post LPS⁶³. However, the small number of miRNA detected in this study strongly suggest that these mechanisms of post-transcriptional regulation may not represent the primary mode by which ethanol alters immune cell functions, at least following *ex vivo* LPS stimulation. In addition to post-transcriptional mechanisms, ethanol has been shown to impact transcriptional mechanisms in the CNS at the genomic level, such as chromatin remodeling^{64–66} and DNA methylation^{67,68}. Future work will focus on identifying changes in chromatin accessibility; patterns of histone methylation and acetylation in purified monocytes and DC subsets to better understand ethanol's impact on immune function.

Overall, our data suggest that moderate and heavy alcohol drinking exert distinct transcriptional and post-transcriptional changes in circulating immune cells. Furthermore, alcohol drinking impacts inflammatory responses to microbial products in a dose-dependent manner. To our knowledge, this is the first comprehensive characterization of alcohol dose-dependent changes in circulating immune cells in the absence of overt organ damage. Given the significant similarity between human and nonhuman primate physiologic and immunologic systems, these findings have a high translational value.

Sample ID	MATRR ID	12 month average ethanol (g/kg/day)	Group	RNA-Seq	Micro RNA-Seq	LPS Stim
MC1	10093	0	Control	X	X	X
MC2	10185	0	Control	X		
MC3	10220	0	Control	X	X	X
MC4	10095	0	Control		X	X
MC5	10184	0	Control		X	X
MM1	10211	2.1	CMD	X		
MM2	10086	2.28	CMD		X	X
MM3	10089	1.95	CMD	X		
MM4	10092	1.85	CMD	X		
MM5	10085	2.07	CMD		X	X
MM6	10084	1.82	CMD	X		
MM7	10087	2.34	CMD		X	X
MM8	10210	1.54	CMD		X	X
MH1	10097	3.01	CHD	X	X	X
MH2	10091	3.09	CHD	X	X	X
MH3	10098	3.32	CHD	X	X	X
MH4	10214	4.21	CHD	X	X	X

Table 1. Summary of animals used in each experiment and drinking behavior in this study.

Methods

Sample collection. Blood samples were collected from 17 male rhesus macaques (average age 6.4 yrs at sample collection), with five animals serving as controls and eight classified as chronic moderate drinkers (CMD) and four as chronic heavy drinkers (CHD) after 12 months of ethanol self-administration through the Monkey Alcohol Tissue Research Resource (www.matrr.com; Supplementary Fig. 1a,b). These cohorts of animals were previously described in detail^{38,69} and leveraged in several immunological studies^{42,44,45}. Differentials from whole blood were obtained using a complete blood count machine calibrated for rhesus blood. Peripheral Blood Mononuclear Cells (PBMC) were isolated by centrifugation over histopaque (Sigma, St Louis, MO) as per manufacturer's protocol and cryopreserved in FetalPlex™ Animal Serum Complex/DMSO until they could be analyzed as a batch. The average daily ethanol dosage for each animal ranged from 1.5 g/kg to 4.2 g/kg as outlined in Table 1. Animals with average daily ethanol consumption <3 g/kg were considered chronic moderate drinkers (CMD) whereas ones with daily consumption >3 g/kg were considered chronic heavy drinkers (CHD). Daily ethanol consumption of individual animals is shown in Supplementary Fig. 1b. A subset of samples was used for each of the analyses as shown in Table 1.

LPS Stimulation assay. A million freshly thawed PBMC were cultured in RPMI supplemented with 10% FBS with or without 100 ng/mL LPS (TLR4 ligand, *E. coli* 055:B5; Invivogen, San Diego CA) for 16 hours in 96-well tissue culture plates at 37 °C in a 5% CO₂ environment. Plates were spun down: supernatants were used to measure production of immune mediators and cell pellets were resuspended in Qiazol (Qiagen, Valencia CA) for RNA extraction. Both cells and supernatants were stored at −80 °C until they could be processed as a batch.

RNA extraction and RNA-Seq library preparation. Total RNA was isolated from PBMC using the mRNAeasy kit (Qiagen, Valencia CA) and quality assessed using Agilent 2100 Bioanalyzer. Following ribosomal RNA depletion using Ribo-Gone rRNA removal kit (Clontech, Mountain View CA), libraries were generated using SMARTer Stranded RNA-Seq kit. Briefly, rRNA depleted RNA was fragmented, converted to double-stranded cDNA and ligated to adapters. The roughly 300bp-long fragments were then amplified by PCR and selected by size exclusion. Libraries were multiplexed and following quality control for size, quality, and concentrations, were sequenced on single-end mode to an average depth of 20 million 100 bp reads.

Small RNA library preparation. Small RNA libraries were generated from total RNA as starting material using QIAseq miRNA Library kit (Qiagen, Valencia CA) per manufacturer's instructions. Total RNA (10 ng) was 3' (1:5 dilution) and 5' adapter (1:2.5) ligated using miRNA specific adapters. Following reverse transcription (adapters 1:5 dilution), cDNA was size selected using QIAseq miRNA NGS beads and PCR amplified for 19 cycles. Following final cleanups, quality and concentrations of the libraries were measured using Bioanalyzer 2100 (Agilent, Santa Clara CA), and size selected to obtain libraries with a target peak 173 bp (average range 145–205 bp) using Pippin Prep (Sage Biosciences, Beverly MA). Final peak sizes and concentration of libraries was verified on the Bioanalyzer. Libraries were sequenced on NextSeq 2500 yielding libraries of 10 million reads each of 75 bp sequenced on single-end mode.

Bioinformatics analysis. RNA-Seq reads were quality checked using FASTQC, adapter and quality trimmed using TrimGalore, retaining reads at least 35 bp long. Reads were aligned to *Macaca mulatta* genome (Mmul_8.0.1) based on annotations available on ENSEMBL (Mmul_8.0.1.92) using TopHat⁷⁰ internally running

Bowtie2. Aligned reads were counted gene-wise using GenomicRanges⁷¹, counting reads in a strand-specific manner. Read counts were normalized using RPKM method for generation of PCA and heatmaps. Pair-wise distances between samples within each group were calculated on raw counts following regularized log transformation using rlog and dist functions in DESeq2. Genes with average raw counts (across all samples) <5 were removed to improve the statistical power of differentially expressed genes. Raw counts were used to identify differentially expressed genes (DEG) using edgeR⁷². DEG are defined as those with at least two-fold change in expression and an FDR controlled at 5%. Only DEG with known macaque gene annotations (protein coding and miRNA precursors) and a minimum median normalized transcript expression (RPKM) of at least 1 were included in all downstream analyses. Functional enrichment of gene expression changes in resting cells was performed using Metascape⁷³ and InnateDB. Networks of functional enrichment terms were generated using Metascape⁷³ and visualized in Cytoscape⁷⁴.

Small RNA reads were trimmed to 15–30 bp range using TrimGalore (www.bioinformatics.babraham.ac.uk/projects/trim_galore/) and aligned to the macaque genome using bowtie2 (-k 50 -very-sensitive-local) using miRNA annotations available on ENSEMBL (Mmul_8.0.1.92). Read counting and differential gene expression was performed as described for RNA-Seq with the exception that genes with $p < 0.05$ were defined as differentially expressed. For all downstream analysis of small RNA regulation, we combined this list of DEG with differentially expressed miRNA precursors detected from bulk RNA-Seq.

ImmGen analysis. Most probable cellular sources of DEG were identified using ImmGen database's (www.immgen.org) "My GeneSet" application, excluding immune cells not typically observed in PBMC. Genes lowly expressed across all cell types were excluded in this analysis.

Analysis of dose-dependent changes using STEM. Dose-based clustering of genes was performed using Short Time-series Expression Miner (STEM) (<http://www.cs.cmu.edu/~jernst/stem/>) using ethanol consumed (g/kg/day) as a continuous variable modeling median normalized transcript levels (RPKM) for every gene as the measured variable. DEG detected following CHD versus controls and CMD versus controls were included in these analyses. Only statistically significant clusters ($p < 0.05$) were retained for downstream interpretation. To measure group differences in identified clusters, gene specific fold change/RPKM were tested for differences using repeated measures one-way ANOVA followed by Holm-Sidak's multiple comparisons test.

mRNA-miRNA Integration. Experimentally validated gene targets of differentially expressed miRNA were identified using miRNet⁷⁵. Only direct mRNA-miRNA interactions were retained and mRNA differentially expressed from RNA-Seq experiment were highlighted using BatchHighlighter option. Functional enrichment of the highlighted genes was tested using miRNet's inbuilt hypergeometric tests ($p < 0.05$) against GO and Reactome databases.

Luminex assay. Circulating immune mediators were measured using nonhuman primate Cytokine/Chemokine/GF (eBioscience, San Diego CA) 29-plex panel measuring levels of cytokines (IFN γ , IL-1 β , IL-2, IL-4, IL-5, IL-6, IL-12, IL-15, IL-17, TNF α , IL-1RA, IL-10, and MIF), chemokines (MCP-1, MIP-1 α , MIP-1 β , RANTES, Eotaxin, MDC, IL-8, MIG, and I-TAC), and growth factors (EGF, FGF, G-CSF, GM-CSF, HGF, and VEGF-A). Standard curves were generated using 5-parameter logistic regression using the xPONENTTM software provided with the MAGPIX instrument (Luminex, Austin TX). Dose-dependent secretion and fold induction were modeled based on g/kg/day ethanol consumed and tested for linear fit using regression analysis in Prism 8 (GraphPad, San Diego CA). Metrics for goodness of fit (r^2) is reported in each figure. P-values were calculated using F-tests testing if the slope was significantly non-zero.

Data visualization. Graphs were generated using several packages in R – dendrograms (DESeq2), venn diagrams (VennDiagram), clustered heatmaps (gplots and lattice), PCA (ggbiplot), 3D-PCA (scatterplot3D), violin plots (ggplot2), beanplots (beanplot). Functional enrichment of overlapping GO terms and protein-protein interactions were visually presented as network images generated in Metascape and Cytoscape. Functional enrichment of standalone GO terms was presented as bar graphs generated in Prism 8. mRNA-microRNA networks were generated in miRNet.

Ethics approval. This study was performed in strict accordance with the recommendations made in the Guide for Care and Use of Laboratory Animals of the National Institutes of Health, the Office of Animal Welfare and the United States Department of Agriculture. The ONPRC Institutional Animal Care and Use Committee approved all animal work.

Data Availability

All small RNA and mRNA sequencing data have been deposited in NCBI's Sequence Read Archive under project accession number PRJNA523863.

References

1. Thakur, L. *et al.* Alcohol consumption and development of acute respiratory distress syndrome: a population-based study. *Int J Environ Res Public Health* **6**, 2426–2435, <https://doi.org/10.3390/ijerph6092426> (2009).
2. Szabo, G. & Bala, S. Alcoholic liver disease and the gut-liver axis. *World J Gastroenterol* **16**, 1321–1329 (2010).
3. Baan, R. *et al.* Carcinogenicity of alcoholic beverages. *Lancet Oncol* **8**, 292–293 (2007).
4. Fedirko, V. *et al.* Alcohol drinking and colorectal cancer risk: an overall and dose-response meta-analysis of published studies. *Ann Oncol* **22**, 1958–1972, <https://doi.org/10.1093/annonc/mdq653> (2011).

5. Grewal, P. & Viswanathan, V. A. Liver cancer and alcohol. *Clin Liver Dis* **16**, 839–850, <https://doi.org/10.1016/j.cld.2012.08.011> (2012).
6. Mukamal, K. J. & Rimm, E. B. Alcohol's effects on the risk for coronary heart disease. *Alcohol Res Health* **25**, 255–261 (2001).
7. Djousse, L., Biggs, M. L., Mukamal, K. J. & Siscovick, D. S. Alcohol consumption and type 2 diabetes among older adults: the Cardiovascular Health Study. *Obesity (Silver Spring)* **15**, 1758–1765, <https://doi.org/10.1038/oby.2007.209> (2007).
8. O'Brien, J. M. Jr. *et al.* Alcohol dependence is independently associated with sepsis, septic shock, and hospital mortality among adult intensive care unit patients. *Crit Care Med* **35**, 345–350, <https://doi.org/10.1097/01.CCM.0000254340.91644.B2> (2007).
9. Schmidt, W. & De Lint, J. Causes of death of alcoholics. *Q J Stud Alcohol* **33**, 171–185 (1972).
10. Saitz, R., Ghali, W. A. & Moskowitz, M. A. The impact of alcohol-related diagnoses on pneumonia outcomes. *Arch Intern Med* **157**, 1446–1452 (1997).
11. Sabot, G. & Vendrame, G. [Incidence of pulmonary tuberculosis in alcoholics. Study based on investigations made at the Ospedale Psichiatrico Provinciale di Udine in the decade 1958–1967]. *Minerva Med* **60**, 5190–5194 (1969).
12. Hudolin, V. Tuberculosis and alcoholism. *Ann N Y Acad Sci* **252**, 353–364 (1975).
13. Kline, S. E., Hedemark, L. L. & Davies, S. F. Outbreak of tuberculosis among regular patrons of a neighborhood bar. *N Engl J Med* **333**, 222–227, <https://doi.org/10.1056/NEJM199507273330404> (1995).
14. Bhattacharya, R. & Shuhart, M. C. Hepatitis C and alcohol: interactions, outcomes, and implications. *J Clin Gastroenterol* **36**, 242–252 (2003).
15. Baum, M. K. *et al.* Alcohol use accelerates HIV disease progression. *AIDS Res Hum Retroviruses* **26**, 511–518, <https://doi.org/10.1089/aid.2009.0211> (2010).
16. Delgado-Rodriguez, M., Gomez-Ortega, A., Mariscal-Ortiz, M., Palma-Perez, S. & Sillero-Arenas, M. Alcohol drinking as a predictor of intensive care and hospital mortality in general surgery: a prospective study. *Addiction* **98**, 611–616 (2003).
17. Pasala, S., Barr, T. & Messaoudi, I. Impact of Alcohol Abuse on the Adaptive Immune System. *Alcohol Res* **37**, 185–197 (2015).
18. Jung, M. K. *et al.* Alcohol exposure and mechanisms of tissue injury and repair. *Alcohol Clin Exp Res* **35**, 392–399, <https://doi.org/10.1111/j.1530-0277.2010.01356.x> (2011).
19. Cohen, S., Tyrrell, D. A., Russell, M. A., Jarvis, M. J. & Smith, A. P. Smoking, alcohol consumption, and susceptibility to the common cold. *Am J Public Health* **83**, 1277–1283 (1993).
20. Takkouche, B. *et al.* Intake of wine, beer, and spirits and the risk of clinical common cold. *Am J Epidemiol* **155**, 853–858 (2002).
21. Ouchi, E. *et al.* Frequent alcohol drinking is associated with lower prevalence of self-reported common cold: a retrospective study. *BMC Public Health* **12**, 987, <https://doi.org/10.1186/1471-2458-12-987> (2012).
22. Cook, R. T. *et al.* Fine T-cell subsets in alcoholics as determined by the expression of L-selectin, leukocyte common antigen, and beta-integrin. *Alcohol Clin Exp Res* **18**, 71–80 (1994).
23. Cook, R. T. *et al.* Modulation of T-cell adhesion markers, and the CD45R and CD57 antigens in human alcoholics. *Alcohol Clin Exp Res* **19**, 555–563 (1995).
24. Cook, R. T. *et al.* Activated CD-8 cells and HLA DR expression in alcoholics without overt liver disease. *J Clin Immunol* **11**, 246–253 (1991).
25. Gonzalez-Quintela, A. *et al.* Serum levels of immunoglobulins (IgG, IgA, IgM) in a general adult population and their relationship with alcohol consumption, smoking and common metabolic abnormalities. *Clin Exp Immunol* **151**, 42–50, <https://doi.org/10.1111/j.1365-2249.2007.03545.x> (2008).
26. Khoruts, A., Stahnke, L., McClain, C. J., Logan, G. & Allen, J. I. Circulating tumor necrosis factor, interleukin-1 and interleukin-6 concentrations in chronic alcoholic patients. *Hepatology* **13**, 267–276 (1991).
27. Barr, T., Helms, C., Grant, K. & Messaoudi, I. Opposing effects of alcohol on the immune system. *Prog Neuropsychopharmacol Biol Psychiatry* **65**, 242–251, <https://doi.org/10.1016/j.pnpbp.2015.09.001> (2016).
28. Bala, S. *et al.* The pro-inflammatory effects of miR-155 promote liver fibrosis and alcohol-induced steatohepatitis. *J Hepatol* **64**, 1378–1387, <https://doi.org/10.1016/j.jhep.2016.01.035> (2016).
29. Mandrekar, P., Bala, S., Catalano, D., Kodys, K. & Szabo, G. The opposite effects of acute and chronic alcohol on lipopolysaccharide-induced inflammation are linked to IRAK-M in human monocytes. *J Immunol* **183**, 1320–1327, <https://doi.org/10.4049/jimmunol.0803206> (2009).
30. Mandrekar, P., Jeliakova, V., Catalano, D. & Szabo, G. Acute alcohol exposure exerts anti-inflammatory effects by inhibiting IκappaB kinase activity and p65 phosphorylation in human monocytes. *J Immunol* **178**, 7686–7693 (2007).
31. Pang, M., Bala, S., Kodys, K., Catalano, D. & Szabo, G. Inhibition of TLR8- and TLR4-induced Type I IFN induction by alcohol is different from its effects on inflammatory cytokine production in monocytes. *BMC Immunol* **12**, 55, <https://doi.org/10.1186/1471-2172-12-55> (2011).
32. Bala, S. *et al.* Induction of Bcl-3 by acute binge alcohol results in toll-like receptor 4/LPS tolerance. *J Leukoc Biol* **92**, 611–620, <https://doi.org/10.1189/jlb.0112050> (2012).
33. Goral, J., Karavitis, J. & Kovacs, E. J. Exposure-dependent effects of ethanol on the innate immune system. *Alcohol* **42**, 237–247, <https://doi.org/10.1016/j.alcohol.2008.02.003> (2008).
34. Gurung, P. *et al.* Chronic ethanol induces inhibition of antigen-specific CD8+ but not CD4+ immunodominant T cell responses following *Listeria monocytogenes* inoculation. *J Leukoc Biol* **85**, 34–43, <https://doi.org/10.1189/jlb.0208101> (2009).
35. Mason, C. M., Dobard, E., Zhang, P. & Nelson, S. Alcohol exacerbates murine pulmonary tuberculosis. *Infect Immun* **72**, 2556–2563 (2004).
36. Meyerholz, D. K. *et al.* Chronic alcohol consumption increases the severity of murine influenza virus infections. *J Immunol* **181**, 641–648 (2008).
37. Mendenhall, C. L., Theus, S. A., Roselle, G. A., Grossman, C. J. & Rouster, S. D. Biphasic *in vivo* immune function after low- versus high-dose alcohol consumption. *Alcohol* **14**, 255–260 (1997).
38. Grant, K. A. *et al.* Drinking typography established by scheduled induction predicts chronic heavy drinking in a monkey model of ethanol self-administration. *Alcohol Clin Exp Res* **32**, 1824–1838, <https://doi.org/10.1111/j.1530-0277.2008.00765.x> (2008).
39. Baker, E. J., Farro, J., Gonzales, S., Helms, C. & Grant, K. A. Chronic alcohol self-administration in monkeys shows long-term quantity/frequency categorical stability. *Alcohol Clin Exp Res* **38**, 2835–2843, <https://doi.org/10.1111/acer.12547> (2014).
40. Jimenez, V. A., Helms, C. M., Cornea, A., Meshul, C. K. & Grant, K. A. An ultrastructural analysis of the effects of ethanol self-administration on the hypothalamic paraventricular nucleus in rhesus macaques. *Front Cell Neurosci* **9**, 260, <https://doi.org/10.3389/fncel.2015.00260> (2015).
41. Helms, C. M. *et al.* A longitudinal analysis of circulating stress-related proteins and chronic ethanol self-administration in cynomolgus macaques. *Alcohol Clin Exp Res* **36**, 995–1003, <https://doi.org/10.1111/j.1530-0277.2011.01685.x> (2012).
42. Messaoudi, I. *et al.* Moderate alcohol consumption enhances vaccine-induced responses in rhesus macaques. *Vaccine* **32**, 54–61, <https://doi.org/10.1016/j.vaccine.2013.10.076> (2013).
43. Asquith, M. *et al.* Chronic ethanol consumption modulates growth factor release, mucosal cytokine production, and microRNA expression in nonhuman primates. *Alcohol Clin Exp Res* **38**, 980–993, <https://doi.org/10.1111/acer.12325> (2014).
44. Barr, T. *et al.* Alcohol Consumption Modulates Host Defense in Rhesus Macaques by Altering Gene Expression in Circulating Leukocytes. *J Immunol* **196**, 182–195, <https://doi.org/10.4049/jimmunol.1501527> (2016).
45. Barr, T. *et al.* Concurrent gut transcriptome and microbiota profiling following chronic ethanol consumption in nonhuman primates. *Gut Microbes*, 1–19, <https://doi.org/10.1080/19490976.2018.1441663> (2018).

46. Sureshchandra, S., Rais, M., Stull, C., Grant, K. & Messaoudi, I. Transcriptome Profiling Reveals Disruption of Innate Immunity in Chronic Heavy Ethanol Consuming Female Rhesus Macaques. *PLoS One* **11**, e0159295, <https://doi.org/10.1371/journal.pone.0159295> (2016).
47. Messaoudi, I., Pasala, S. & Grant, K. Could moderate alcohol intake be recommended to improve vaccine responses? *Expert Rev Vaccines* **13**, 817–819, <https://doi.org/10.1586/14760584.2014.924405> (2014).
48. Ernst, J. & Bar-Joseph, Z. STEM: a tool for the analysis of short time series gene expression data. *BMC Bioinformatics* **7**, 191, <https://doi.org/10.1186/1471-2105-7-191> (2006).
49. Heng, T. S. & Painter, M. W. Immunological Genome Project, C. The Immunological Genome Project: networks of gene expression in immune cells. *Nat Immunol* **9**, 1091–1094, <https://doi.org/10.1038/ni1008-1091> (2008).
50. Delgado-Rodriguez, M. *et al.* Alcohol consumption and the risk of nosocomial infection in general surgery. *Br J Surg* **90**, 1287–1293, <https://doi.org/10.1002/bjs.4186> (2003).
51. Ballard, H. S. The hematological complications of alcoholism. *Alcohol Health Res World* **21**, 42–52 (1997).
52. Shi, X., Lin, Y. P., Gao, B. & Zhang, P. Impairment of Hematopoietic Precursor Cell Activation during the Granulopoietic Response to Bacteremia in Mice with Chronic-Plus-Binge Alcohol Administration. *Infect Immun* **85**, <https://doi.org/10.1128/IAI.00369-17> (2017).
53. Gaydos, J. *et al.* Alcohol abuse and smoking alter inflammatory mediator production by pulmonary and systemic immune cells. *Am J Physiol Lung Cell Mol Physiol* **310**, L507–518, <https://doi.org/10.1152/ajplung.00242.2015> (2016).
54. Friberg, D., Bryant, J., Shannon, W. & Whiteside, T. L. *In vitro* cytokine production by normal human peripheral blood mononuclear cells as a measure of immunocompetence or the state of activation. *Clin Diagn Lab Immunol* **1**, 261–268 (1994).
55. Liangpunsakul, S. *et al.* Quantity of alcohol drinking positively correlates with serum levels of endotoxin and markers of monocyte activation. *Sci Rep* **7**, 4462, <https://doi.org/10.1038/s41598-017-04669-7> (2017).
56. Purohit, V. *et al.* Alcohol, intestinal bacterial growth, intestinal permeability to endotoxin, and medical consequences: summary of a symposium. *Alcohol* **42**, 349–361, <https://doi.org/10.1016/j.alcohol.2008.03.131> (2008).
57. Wang, Y. *et al.* Effects of alcohol on intestinal epithelial barrier permeability and expression of tight junction-associated proteins. *Mol Med Rep* **9**, 2352–2356, <https://doi.org/10.3892/mmr.2014.2126> (2014).
58. Bala, S., Marcos, M., Gattu, A., Catalano, D. & Szabo, G. Acute binge drinking increases serum endotoxin and bacterial DNA levels in healthy individuals. *PLoS One* **9**, e96864, <https://doi.org/10.1371/journal.pone.0096864> (2014).
59. Iyer, S. S. & Cheng, G. Role of interleukin 10 transcriptional regulation in inflammation and autoimmune disease. *Crit Rev Immunol* **32**, 23–63 (2012).
60. Zhang, X. *et al.* TLR4/ROS/miRNA-21 pathway underlies lipopolysaccharide instructed primary tumor outgrowth in lung cancer patients. *Oncotarget* **7**, 42172–42182, <https://doi.org/10.18632/oncotarget.9902> (2016).
61. Yuan, H., Ma, J., Li, T. & Han, X. MiR-29b aggravates lipopolysaccharide-induced endothelial cells inflammatory damage by regulation of NF- κ B and JNK signaling pathways. *Biomed Pharmacother* **99**, 451–461, <https://doi.org/10.1016/j.biopha.2018.01.060> (2018).
62. Koga, T. *et al.* MicroRNA-204-3p inhibits lipopolysaccharide-induced cytokines in familial Mediterranean fever via the phosphoinositide 3-kinase gamma pathway. *Rheumatology (Oxford)* **57**, 718–726, <https://doi.org/10.1093/rheumatology/kex451> (2018).
63. Okugawa, S. *et al.* Janus kinase 2 is involved in lipopolysaccharide-induced activation of macrophages. *Am J Physiol Cell Physiol* **285**, C399–408, <https://doi.org/10.1152/ajpcell.00026.2003> (2003).
64. Pandey, S. C., Ugale, R., Zhang, H., Tang, L. & Prakash, A. Brain chromatin remodeling: a novel mechanism of alcoholism. *J Neurosci* **28**, 3729–3737, <https://doi.org/10.1523/JNEUROSCI.5731-07.2008> (2008).
65. Qiang, M., Denny, A., Lieu, M., Carreon, S. & Li, J. Histone H3K9 modifications are a local chromatin event involved in ethanol-induced neuroadaptation of the NR2B gene. *Epigenetics* **6**, 1095–1104, <https://doi.org/10.4161/epi.6.9.16924> (2011).
66. Ponomarev, I., Wang, S., Zhang, L., Harris, R. A. & Mayfield, R. D. Gene coexpression networks in human brain identify epigenetic modifications in alcohol dependence. *J Neurosci* **32**, 1884–1897, <https://doi.org/10.1523/JNEUROSCI.3136-11.2012> (2012).
67. Marutha Ravindran, C. R., Mehta, A. K. & Ticku, M. K. Effect of chronic administration of ethanol on the regulation of the delta-subunit of GABA(A) receptors in the rat brain. *Brain Res* **1174**, 47–52, <https://doi.org/10.1016/j.brainres.2007.07.077> (2007).
68. Manzardo, A. M., Henkhaus, R. S. & Butler, M. G. Global DNA promoter methylation in frontal cortex of alcoholics and controls. *Gene* **498**, 5–12, <https://doi.org/10.1016/j.gene.2012.01.096> (2012).
69. Allen, D. C., Gonzales, S. W. & Grant, K. A. Effect of repeated abstinence on chronic ethanol self-administration in the rhesus monkey. *Psychopharmacology (Berl)* **235**, 109–120, <https://doi.org/10.1007/s00213-017-4748-9> (2018).
70. Trapnell, C. *et al.* Differential gene and transcript expression analysis of RNA-seq experiments with TopHat and Cufflinks. *Nat Protoc* **7**, 562–578, <https://doi.org/10.1038/nprot.2012.016> (2012).
71. Lawrence, M. *et al.* Software for computing and annotating genomic ranges. *PLoS Comput Biol* **9**, e1003118, <https://doi.org/10.1371/journal.pcbi.1003118> (2013).
72. Robinson, M. D., McCarthy, D. J. & Smyth, G. K. edgeR: a Bioconductor package for differential expression analysis of digital gene expression data. *Bioinformatics* **26**, 139–140, <https://doi.org/10.1093/bioinformatics/btp616> (2010).
73. Tripathi, S. *et al.* Meta- and Orthogonal Integration of Influenza “OMICs” Data Defines a Role for UBR4 in Virus Budding. *Cell Host Microbe* **18**, 723–735, <https://doi.org/10.1016/j.chom.2015.11.002> (2015).
74. Demchak, B. *et al.* Cytoscape: the network visualization tool for GenomeSpace workflows. *F1000Res* **3**, 151, <https://doi.org/10.12688/f1000research.4492.2> (2014).
75. Fan, Y. *et al.* miRNet - dissecting miRNA-target interactions and functional associations through network-based visual analysis. *Nucleic Acids Res* **44**, W135–141, <https://doi.org/10.1093/nar/gkw288> (2016).

Acknowledgements

The authors wish to thank the members of the Grant laboratory for animal husbandry and sample collection. This work has been funded by NIH 8P51 ODO11092-533, NIH/NIAAA R24AA019431, U01 AA13641, U01 AA13510 and NIH/NIAAA R21AA021947 and R21AA025839. We thank Alexander Badten and Hankun Liu for assistance with preparation of sequencing libraries.

Author Contributions

I.M. and K.G. designed the study. S.S., A.J., A.R., N.N. and N.W. performed the experiments. S.S. and B.L. analyzed the data. S.S., I.M. and K.G. wrote the manuscript. All authors have read the final version of the manuscript.

Additional Information

Supplementary information accompanies this paper at <https://doi.org/10.1038/s41598-019-44302-3>.

Competing Interests: The authors declare no competing interests.

Publisher's note: Springer Nature remains neutral with regard to jurisdictional claims in published maps and institutional affiliations.



Open Access This article is licensed under a Creative Commons Attribution 4.0 International License, which permits use, sharing, adaptation, distribution and reproduction in any medium or format, as long as you give appropriate credit to the original author(s) and the source, provide a link to the Creative Commons license, and indicate if changes were made. The images or other third party material in this article are included in the article's Creative Commons license, unless indicated otherwise in a credit line to the material. If material is not included in the article's Creative Commons license and your intended use is not permitted by statutory regulation or exceeds the permitted use, you will need to obtain permission directly from the copyright holder. To view a copy of this license, visit <http://creativecommons.org/licenses/by/4.0/>.

© The Author(s) 2019